Proceeding of the IEEE
International Conference on Robotics and Biomimetics
Dali, China, December 2019

Stable Gait Generation of Impaired Biped Robot with Reaction Wheel

Cong Yan, Fumihiko Asano
School of Information Science
Japan Advanced Institute of Science and Technology
Ishikawa, Japan
{*gansou315, fasano*}*@jaist.ac.jp*

Longchuan Li
Research Organization of Science and Technology
Ritsumeikan University
1-1-1 Nojihigashi, Kusatsu, Shiga
lltt2144@fc.ritsumei.ac.jp

***Abstract*— In this paper, we propose two methods for stable gait generation of a biped robot with damaged motor on one-side. First, we derive the dynamics and control method. Only single control torque between the hip and one leg is applied by reaction wheel or one more reaction wheel act on damaged leg. Second, we numerically show the period-2 gait of this dynamic walking. Finally, the gait properties are analyzed via parametric study. The results show that by adjusting the target control time for the actuated swing/stance leg separately and appropriately with only one input, the impaired biped robot can walk steadily. Add one more reaction wheel on the damaged leg, Not only steady-state gait of the robot can be generated, but also its stride length and walking speed can be controlled. Consequently, the potential barrier can be overcome successfully.**

***Index Terms*— Point-footed biped, Reaction wheel, Limit cycle, Rehabilitation.**

I. Introduction

There have been many studies of various legged robots. Multi-legged robots such as four-legged walking have the advantage of high stability. On the other hand, the biped robot can generate gait close to human, so it is considered that it can be applied to various road surfaces. With these considerations, Asano suggests a method for generating an underactuated bipedal gait completing in one step in the presence of an upper body that behaves as zero dynamics [1]. A method for generating an underactuated bipedal gait without including state jumps during motion by using a reaction wheel attached to the hip joint [2]. In recent years, biped robots such as ASIMO [3] and ATLAS [4] have been designed and developed, but they use many actuators and sensors, caused energy loss and control complexity etc. Another major problem is that the walking function is lost when the actuator on one side fails. Brown and Schmiedeler proved the effectiveness of using reaction wheel to control the balance of robots [5]. Admittedly, as a result of increasing the weight of the wheel, there will be more energy loss in the system. Due to the special driving mode of the reaction wheel, It can extend the range of feasible periodic gait and the energy efficiency can be improved [6], so the energy loss can be offset [7], however the reaction wheel is only used to assist the robot to walk more efficiently, and the main actuators are the motors between the joints. In the condition

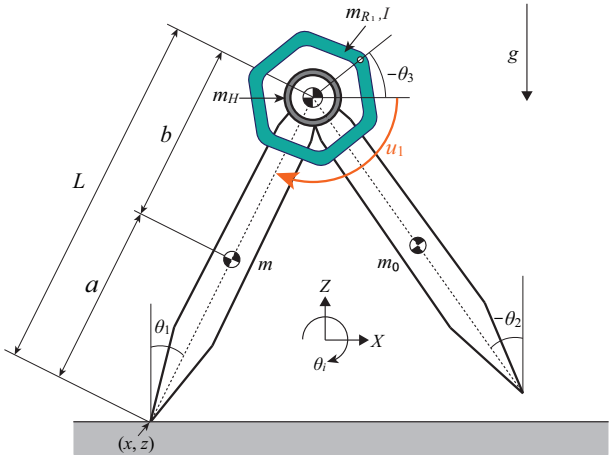

Fig. 1. Biped walking robot model with single reaction wheel

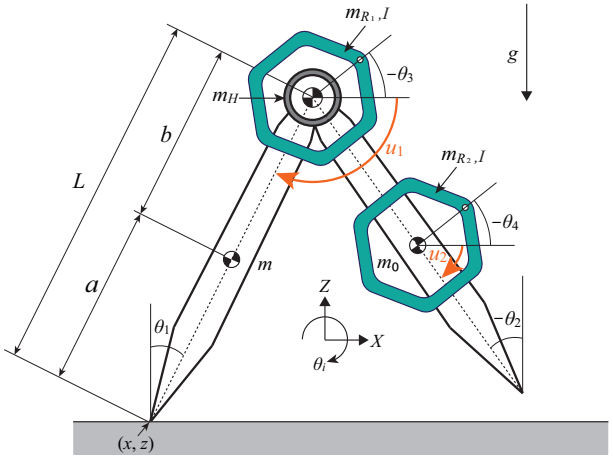

Fig. 2. 5 Biped walking robot model with double reaction wheels

978-1-7281-6321-5/19//$31.00 ©2019 IEEE

of the motor of one leg is invalid, whether it is possible to drive the other leg to walk stably only through the reaction wheel at the waist, and whether it can walk more efficiently and steadily with a reaction wheel on the damaged leg.

To answer this question, in this paper, we consider the stable gait generation problem when one leg is passive in two models contains two legs and single reaction wheel on waist or double reaction wheels on waist and passive leg. Therefore, we propose two methods of gait generation by using reaction wheels. In Fig. 1, refer to the concept of passive walking [8] [9], it is known that the damaged leg is projected forward like a pendulum using gravity and inertia force, it can walk steadily with only single input. Compared with Fig. 1, the Fig. 2 contains one more reaction wheel on damaged leg, we can control the walking distance and speed. In addition, we show that stable gait generation and control of walking distance and speed is possible by applying multi-period input by the proposed method through numerical simulation.

II. Models of Biped Robots

A. Equation of Motion

Fig.1 illustrates the 5-DOF 1-input biped walking robot model. This robot has a waist with a mass of m_H [kg]. Two identical rigid leg frame with a length of $L(=a+b)$ [m] and a mass of $m(=m_0)$ [kg]. In addition, It has a reaction wheel with a mass of m_{R1} [kg] and the inertial moment about it is I [$\mathrm{kg}\cdot\mathrm{m}^2$]. Here, (x,z) is the tip position of the stance leg. θ_1 [rad], θ_2 [rad] is the angular position of the stance leg and swing leg regard to vertical. θ_3 [rad] is the angular position of the reaction wheel regard to horizontal. The motor between one leg and the hip joint is damaged. The u_1 is the the only possible control input. Moreover, the inertial moment of the leg rest and the friction of the hip joint are ignored.

Compared with Fig. 1, Fig. 2 just adds a reaction wheel to the damaged leg. The reaction wheel with a mass of m_{R2} [kg] and the inertial moment about it is I [$\mathrm{kg}\cdot\mathrm{m}^2$]. θ_4 [rad] is the angular position of the reaction wheel regard to horizontal. So this robot illustrates the 6-DOF 2-input biped walking robot model.

$\boldsymbol{q}_1 = \begin{bmatrix} x & z & \theta_1 & \theta_2 & \theta_3 \end{bmatrix}^{\mathrm{T}}$ and $\boldsymbol{q}_2 = \begin{bmatrix} x & z & \theta_1 & \theta_2 & \theta_3 & \theta_4 \end{bmatrix}^{\mathrm{T}}$ are the generalized coordinate vectors about Fig. 1 and Fig.2. The robot equation of motion then becomes

$$\boldsymbol{M}\ddot{\boldsymbol{q}} + \boldsymbol{h} = \boldsymbol{J}^{\mathrm{T}}\boldsymbol{\lambda} + \boldsymbol{S}\boldsymbol{u}, \tag{1}$$

$$\boldsymbol{J}\dot{\boldsymbol{q}} = \boldsymbol{0}_{2\times 1}, \tag{2}$$

where $\boldsymbol{M}$ represents the inertia matrix, $\boldsymbol{h}$ represents the combination of central force, Coriolis force and gravity terms. On the right-hand side, and $\boldsymbol{J}^{\mathrm{T}}\boldsymbol{\lambda}$ is the holonomic constraint. In addition, u_1 is the first control input by reaction wheel between one leg and hip, u_2 is the second control input between another leg and reaction wheel.

The driving vector

$$\boldsymbol{S}_{11} = \begin{bmatrix} 0 & 0 & 1 & 0 & -1 \end{bmatrix}^{\mathrm{T}}, \tag{3}$$

$$\boldsymbol{S}_{12} = \begin{bmatrix} 0 & 0 & 0 & 1 & -1 \end{bmatrix}^{\mathrm{T}}, \tag{4}$$

and

$$\boldsymbol{S}_{21} = \begin{bmatrix} 0 & 0 & 1 & 0 & -1 & 0 \\ 0 & 0 & 0 & 1 & 0 & -1 \end{bmatrix}^{\mathrm{T}}, \tag{5}$$

$$\boldsymbol{S}_{22} = \begin{bmatrix} 0 & 0 & 0 & 1 & -1 & 0 \\ 0 & 0 & 1 & 0 & 0 & -1 \end{bmatrix}^{\mathrm{T}}, \tag{6}$$

are respectively about Fig. 1 and Fig. 2. When the active leg (means the reaction wheel between the leg and the hip is controllable) is the stance leg, set the driving vector to $\boldsymbol{S}_{11}$ or $\boldsymbol{S}_{21}$. Contrary, when the semi-active leg is the stance leg, set the driving vector to $\boldsymbol{S}_{12}$ or $\boldsymbol{S}_{22}$.

The velocity constraints of the contact position of the stance leg and the ground on a non-slip plane are specified as

$$\dot{x} = 0, \quad \dot{z} = 0. \tag{7}$$

Therefore, Jacobians $\boldsymbol{J}$ are determined as

$$\boldsymbol{J}_1 = \begin{bmatrix} 1 & 0 & 0 & 0 & 0 \\ 0 & 1 & 0 & 0 & 0 \end{bmatrix}, \tag{8}$$

and

$$\boldsymbol{J}_2 = \begin{bmatrix} 1 & 0 & 0 & 0 & 0 & 0 \\ 0 & 1 & 0 & 0 & 0 & 0 \end{bmatrix}. \tag{9}$$

The ground reaction force $\boldsymbol{\lambda}$ [N] is the simultaneous solution of Eqs. (1) and (2):

$$\begin{aligned} \boldsymbol{\lambda} &= -\boldsymbol{X}^{-1}\boldsymbol{J}\boldsymbol{M}^{-1}(\boldsymbol{S}\boldsymbol{u} - \boldsymbol{h}), \\ \boldsymbol{X} &:= \boldsymbol{J}\boldsymbol{M}^{-1}\boldsymbol{J}^{\mathrm{T}}. \end{aligned} \tag{10}$$

Positive ground reaction force is required to generate stable locomotion. By substituting Eq. (10) into Eq. (1), we obtain

$$\begin{aligned} \ddot{\boldsymbol{q}} &= \boldsymbol{M}^{-1}\boldsymbol{Y}(\boldsymbol{S}\boldsymbol{u} - \boldsymbol{h}), \\ \boldsymbol{Y} &:= \boldsymbol{I}_{5\mathrm{or}6} - \boldsymbol{J}^{\mathrm{T}}\boldsymbol{X}^{-1}\boldsymbol{J}\boldsymbol{M}^{-1}, \end{aligned} \tag{11}$$

where $\boldsymbol{I}_{5\mathrm{or}6}$ is the identity matrix of size 5 or 6.

B. Equation of Collision

In this paper, we assume that the rear leg crawls on the ground immediately after the collision according to the inelastic collision model, and the state transition is as follows

$$\boldsymbol{M}\dot{\boldsymbol{q}}^{+} = \boldsymbol{M}\dot{\boldsymbol{q}}^{-} + \boldsymbol{J}_I^{\mathrm{T}}\boldsymbol{\lambda}_I, \tag{12}$$

$$\boldsymbol{J}_I\dot{\boldsymbol{q}}^{+} = \boldsymbol{0}_{2\times 1}. \tag{13}$$

Here, the superscripts "$-$" and "$+$" mean immediately before and immediately after a collision. The velocity constraint condition for the landing point of the forefoot is determined as

$$\dot{x}^{+} = 0, \quad \dot{z}^{+} = 0. \tag{14}$$

These are detailed as

$$\frac{\mathrm{d}}{\mathrm{d}t}\begin{bmatrix}\bar{x}\\ \bar{z}\end{bmatrix}^{+} = \frac{\mathrm{d}}{\mathrm{d}t}\begin{bmatrix}x+L\sin\theta_1-L\sin\theta_2\\ z+L\cos\theta_1-L\cos\theta_2\end{bmatrix}^{+} = \begin{bmatrix}1 & 0 & L\cos\theta_1^- & -L\cos\theta_2^- & 0 & (0)\\ 0 & 1 & -L\sin\theta_1^- & L\sin\theta_2^- & 0 & (0)\end{bmatrix}\dot{\boldsymbol{q}}^{+} \quad (15)$$

Here, "()" means applicable to Fig. 2, the same applies to the following. Therefore, we obtain

$$\boldsymbol{J}_I^{\mathrm{T}} = \begin{bmatrix}1 & 0\\ 0 & 1\\ L\cos\theta_1^- & -L\sin\theta_1^-\\ -L\cos\theta_2^- & L\sin\theta_2^-\\ 0 & 0\\ (0) & (0)\end{bmatrix}. \quad (16)$$

By solving the simultaneous Eqs. (12) and (13), Lagrange multiplier vector $\boldsymbol{\lambda}_I \in \mathbb{R}^2$ can be derived as

$$\begin{aligned}\boldsymbol{\lambda}_I &= -\boldsymbol{X}_I^{-1}\boldsymbol{J}_I\dot{\boldsymbol{q}}^{-}, \quad (17)\\ \boldsymbol{X}_I &:= \boldsymbol{J}_I\boldsymbol{M}^{-1}\boldsymbol{J}_I^{\mathrm{T}}.\end{aligned}$$

By substituting Eq. (17) into Eq. (12), we obtain

$$\dot{\boldsymbol{q}}^{+} = \left(\boldsymbol{I}_{5\mathrm{or}6} - \boldsymbol{M}^{-1}\boldsymbol{J}_I^{\mathrm{T}}\boldsymbol{X}_I^{-1}\boldsymbol{J}_I\right)\dot{\boldsymbol{q}}^{-}. \quad (18)$$

For the expression (18), we need to reset $\dot{\boldsymbol{q}}^{+}$ as

$$\dot{\boldsymbol{q}}^{+} = \begin{bmatrix}\dot{x}^{+}+L\dot{\theta}_1^{+}\cos\theta_1^{-}-L\dot{\theta}_2^{+}\cos\theta_2^{-}\\ \dot{z}^{+}-L\dot{\theta}_1^{+}\sin\theta_1^{-}+L\dot{\theta}_2^{+}\sin\theta_2^{-}\\ \dot{\theta}_2^{+}\\ \dot{\theta}_1^{+}\\ \dot{\theta}_3^{+}\\ (\dot{\theta}_4^{+})\end{bmatrix}. \quad (19)$$

On the other hand, $\boldsymbol{q}^{+}$ is reset as

$$\boldsymbol{q}^{+} = \begin{bmatrix}x^{-}+L\sin\theta_1^{-}-L\sin\theta_2^{-}\\ z^{-}+L\cos\theta_1^{-}-L\cos\theta_2^{-}\\ \theta_2^{-}\\ \theta_1^{-}\\ \theta_3^{-}\\ (\theta_4^{-})\end{bmatrix}. \quad (20)$$

III. Control Methods

We need to control the active leg with the hip joint in Fig. 1. We also need to use the reaction wheel to control the angular position of the semi-active leg regard to vertical in Fig. 2. Let $\boldsymbol{y}_1 = \boldsymbol{C}_1\boldsymbol{q}$ and $\boldsymbol{y}_2 = \boldsymbol{C}_2\boldsymbol{q}$ be the control output: $\boldsymbol{C}_1 = \boldsymbol{C}_{11}$ or $\boldsymbol{C}_{12}$ (about Fig. 1) and $\boldsymbol{C}_2 = \boldsymbol{C}_{21}$ or $\boldsymbol{C}_{22}$ (about Fig. 2) where

$$\boldsymbol{C}_{11} = \boldsymbol{S}_{11} = \begin{bmatrix}0 & 0 & 1 & 0 & -1\end{bmatrix}, \quad (21)$$

$$\boldsymbol{C}_{12} = \boldsymbol{S}_{12} = \begin{bmatrix}0 & 0 & 0 & 1 & -1\end{bmatrix}, \quad (22)$$

and

$$\boldsymbol{C}_{21} = \begin{bmatrix}0 & 0 & 1 & 0 & 0 & 0\\ 0 & 0 & 0 & 1 & 0 & 0\end{bmatrix}, \quad (23)$$

$$\boldsymbol{C}_{22} = \begin{bmatrix}0 & 0 & 0 & 1 & 0 & 0\\ 0 & 0 & 1 & 0 & 0 & 0\end{bmatrix}. \quad (24)$$

When the active leg is the stance leg, we use the $\boldsymbol{C}_{11}$ or $\boldsymbol{C}_{21}$ to control the robot walking. Contrary, when the semi-active leg is the stance leg, we set to $\boldsymbol{C}_{12}$ or $\boldsymbol{C}_{22}$. The second order derivative of $y(t)$ with respect to time becomes

$$\ddot{y} = \boldsymbol{C}\ddot{\boldsymbol{q}} = \boldsymbol{C}\boldsymbol{M}^{-1}\boldsymbol{Y}(\boldsymbol{S}\boldsymbol{u}-\boldsymbol{h}) = A\boldsymbol{u}-B, \quad (25)$$

where

$$A := \boldsymbol{C}\boldsymbol{M}^{-1}\boldsymbol{Y}\boldsymbol{S} \quad \text{and} \quad B := \boldsymbol{C}\boldsymbol{M}^{-1}\boldsymbol{Y}\boldsymbol{h}.$$

Realization of $y \equiv y_{\mathrm{d}}(t)$ by strict output following control. In order to specify the position, velocity and acceleration of the initial and terminal states as a total of six boundary conditions and to enable periodic and smooth tracking, the desired trajectory between the active leg and the upper body, the semi-active leg and the reaction wheel need to use a 5th-order function and let t be time parameter that is reset to zero during stance leg exchange, each boundary condition is as follows.

$$\begin{aligned}y_{\mathrm{d}}(0) &= -\frac{\alpha}{2}, \quad \dot{y}_{\mathrm{d}}(0) = 0, \quad \ddot{y}_{\mathrm{d}}(0) = 0\\ y_{\mathrm{d}}(T_{\mathrm{set}}) &= \frac{\alpha}{2}, \quad \dot{y}_{\mathrm{d}}(T_{\mathrm{set}}) = 0, \quad \ddot{y}_{\mathrm{d}}(T_{\mathrm{set}}) = 0\end{aligned}$$

Here, $-\alpha/2$ [rad] is the initial angle, and T_{set} [s] is the end time of each single support period. By solving this, we get

$$a_0 = -\frac{\alpha}{2}, \quad a_3 = \frac{10\alpha}{T_{\mathrm{set}}^3}, \quad a_4 = -\frac{15\alpha}{T_{\mathrm{set}}^4}, \quad a_5 = \frac{6\alpha}{T_{\mathrm{set}}^5}.$$

Set the desired trajectory as

$$y_{\mathrm{d}}(t) = -\frac{\alpha}{2} + \alpha\left(\frac{6t^5}{T_{\mathrm{set}}^5} - \frac{15t^4}{T_{\mathrm{set}}^4} + \frac{10t^3}{T_{\mathrm{set}}^3}\right). \quad (26)$$

TABLE I
Physical and Control Parameters

Symbol	Value	Unit
m_H	10	kg
m	5	kg
m_0	5	kg
m_{R1}	1	kg
m_{R2}	1	kg
a	0.5	m
b	0.5	m
L	1	m
I	0.1	kg·m^2

Symbol	Value	Unit
$T_{\mathrm{set}}^{\mathrm{a}}$	0.3	s
$T_{\mathrm{set}}^{\mathrm{s}}$	0.75	s
$T_{\mathrm{set1}}^{\mathrm{a}}$	0.3	s
$T_{\mathrm{set1}}^{\mathrm{s}}$	0.35	s
$T_{\mathrm{set2}}^{\mathrm{a}}$	0.3	s
$T_{\mathrm{set2}}^{\mathrm{s}}$	0.35	s
g	9.81	m/s^2
K_D	40	s^{-2}
K_P	400	s^{-1}

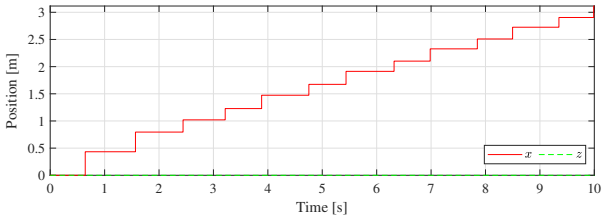

(a) Position

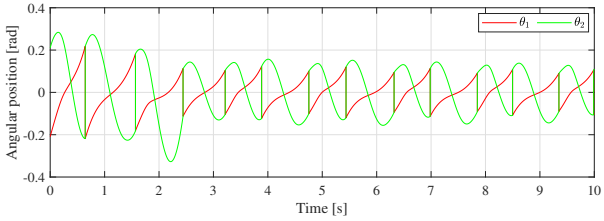

(b) Angular position

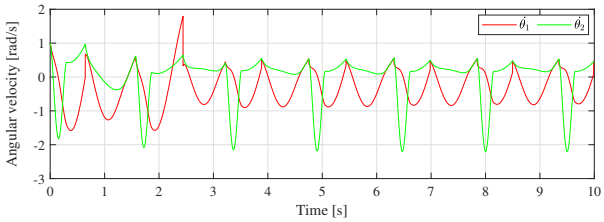

(c) Angular velocity

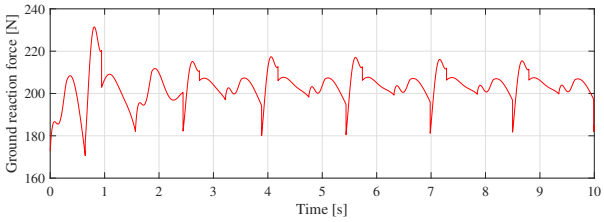

(d) Vertical ground reaction force

Fig. 3. Simulation results where $T^{\mathrm{a}}_{\mathrm{set}}$=0.3 [s] and $T^{\mathrm{s}}_{\mathrm{set}}$=0.75 [s]

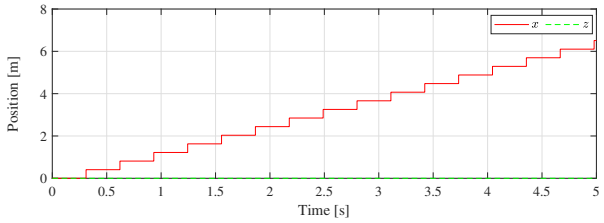

(a) Position

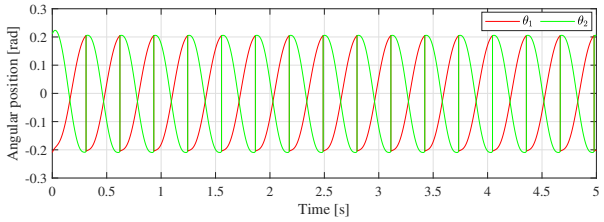

(b) Angular position

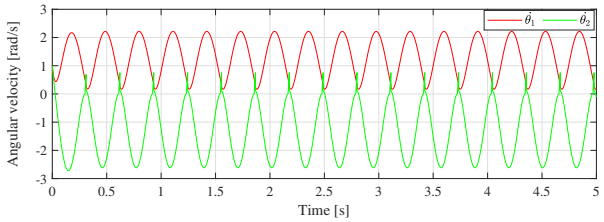

(c) Angular velocity

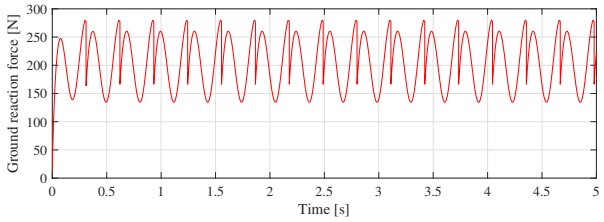

(d) Vertical ground reaction force

Fig. 4. Simulation results where $T^{\mathrm{a}}_{\mathrm{set1}}$=0.3 [s], $T^{\mathrm{s}}_{\mathrm{set1}}$=0.35 [s], $T^{\mathrm{a}}_{\mathrm{set2}}$=0.3 [s] and $T^{\mathrm{s}}_{\mathrm{set2}}$=0.35 [s]

Consequently, the control input for achieeving $y(t) \to y_{\mathrm{d}}(t)$ is defined as

$$u = A^{-1}(v+B), \tag{27}$$
$$v = \ddot{y}_{\mathrm{d}}(t) + K_D(\dot{y}_{\mathrm{d}}(t) - \dot{y}) + K_P(y_{\mathrm{d}}(t) - y), \tag{28}$$

where K_{D} [s^{-2}] and K_{P} [s^{-1}] are the PD control gains.

In Fig. 1, if the active leg is a stance leg, set target time T_{set} to $T^{\mathrm{a}}_{\mathrm{set}}$. If the semi-active leg is a swing leg, set target time T_{set} to $T^{\mathrm{s}}_{\mathrm{set}}$. Empathy, in Fig. 2, if the active leg is a stance leg, set target time T_{set} to $T^{\mathrm{a}}_{\mathrm{set1}}$, else set to $T^{\mathrm{a}}_{\mathrm{set2}}$. If the semi-active leg is a swing leg, set target time T_{set} to $T^{\mathrm{s}}_{\mathrm{set1}}$, else set to $T^{\mathrm{s}}_{\mathrm{set2}}$. By properly adjusting the T_{set}, the stable gait generation becomes possible.

IV. Simulation Results

We use the parameters listed in Table I to conduct following process. In Fig. 1, Set the target angular between active leg and reaction wheel on waist is $\alpha_1/2 = 0.209$ [rad]. In Fig. 2, Set the target angular between active leg and semi-active leg egard to vertical are $\alpha_2/2 = 0.209$ [rad]. Set the initial conditions as

$$\boldsymbol{q}(0) = \begin{bmatrix} 0 & 0 & -0.209 & 0.210 & 0 & (0) \end{bmatrix}^{\mathrm{T}},$$
$$\dot{\boldsymbol{q}}(0) = \begin{bmatrix} 0 & 0 & 1 & 1 & 1 & (1) \end{bmatrix}^{\mathrm{T}}.$$

Therefore, walking starts from the state immediately after the leg collides with sufficient kinetic energy.

Fig. 3 shows the simulation results of generated motion about the model of Fig. 1 where $T^{\mathrm{a}}_{\mathrm{set}}$=0.3 [s], $T^{\mathrm{s}}_{\mathrm{set}}$=0.75 [s].

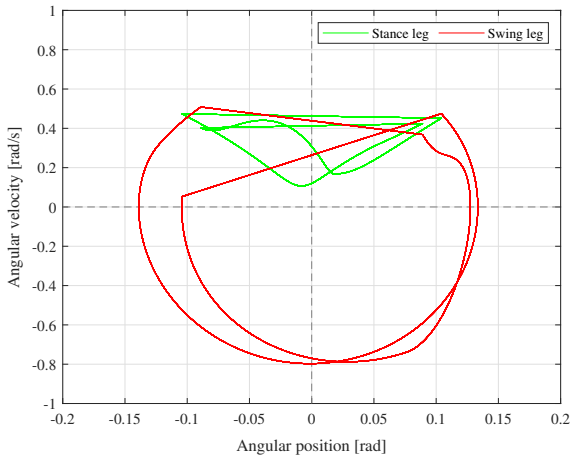

Fig. 5. Phase-plane plot of generated motion where T^{a}_{set}=0.3 [s] and T^{s}_{set}=0.75 [s]

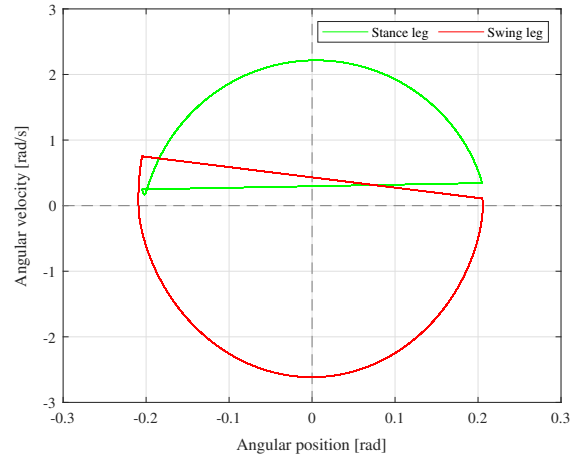

Fig. 6. Phase-plane plot of generated motion where T^{a}_{set1}=0.3 [s], T^{s}_{set1}=0.35 [s], T^{a}_{set2}=0.3 [s] and T^{s}_{set2}=0.35 [s]

Since only one input is effective, it is considered that the generation of the stable gait is considerably severe. Here, we have to adjust the T_{set} to get the stable gait, and the T^{a}_{set} and T^{s}_{set} can not be the same time like a normal biped robot.

Here, (a) is the tip position of the stance leg, (b) is the angular positions, (c) is the angular velocities, and (d) is the vertical ground reaction force. As seen from x in the Fig. 3 (a), due to the fact that only the angular between active leg and reaction wheel is contolled to vertical, the state of walking advances forward alternately with long and short periods. We can see that the robot has a larger distance in the first few steps, and then becomes smaller and tends to be stable from Fig. 3(b). It can be seen from Fig. 3(c) that the angular velocity at this time is cyclically affected. From Fig. 3 (d), we can also see that the vertical ground reaction force always kept positive.

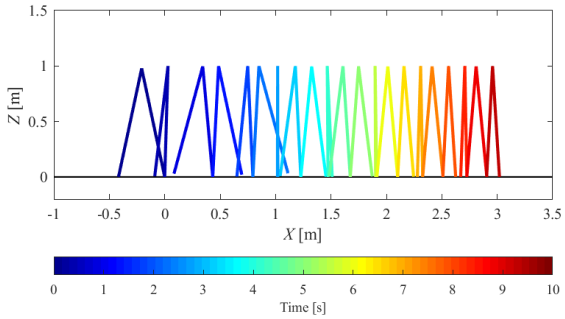

Fig. 7. Stick diagram of the robot where T^{a}_{set}=0.3 [s] and T^{s}_{set}=0.75 [s]

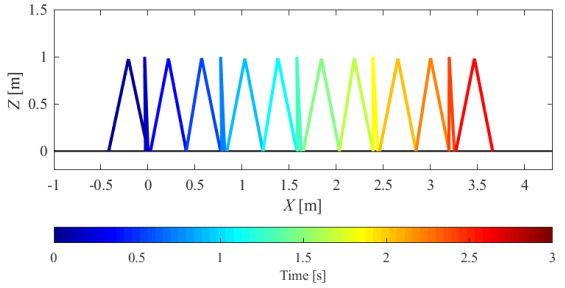

Fig. 8. Stick diagram of the robot where T^{a}_{set1}=0.3 [s], T^{s}_{set1}=0.35 [s], T^{a}_{set2}=0.3 [s] and T^{s}_{set2}=0.35 [s]

Fig. 4 shows the simulation results of generated motion about Fig. 2 where T^{a}_{set1}=0.3 [s], T^{s}_{set1}=0.35 [s], T^{a}_{set2}=0.3 [s] and T^{s}_{set2}=0.35 [s]. Compared to Fig. 3, we also adjust the T_{set} to get the more stable gait, but the adjustment of T_{set} is not so difficult like Fig. 3, so we can adjust the T_{set} relatively freely. As seen from x in the Fig. 3 (a), due to the fact that the angular between reaction wheel and active leg or semi-active leg are both contolled to vertical, we can control the equal walking distance at each step. It can be seen from Fig. 3(c) that the angular velocity at this time is cyclically affected and the walking speed is the same.

In order to verify the stability of movement, Fig. 5 shows a phase-plan plot of the gait about Fig. 1 after a sufficient time (250 [s]). The results show that the motion converges to a stationary limit cycle of 2 cycles. We can see that the swing of the stance leg is significantly smaller than that of the swing leg. Fig. 6 shows a phase-plan plot of the gait about Fig. 2, also after a sufficient time (250 [s]). The results show that the motion almost converges to the stationary limit cycle of 1 cycle.

Fig. 7 shows the stick diagram of the stance leg and swing leg about Fig. 1, due to the T^{s}_{set} is slightly longer than T^{a}_{set}, the walking is slightly slower. Only one leg has input with the reaction wheel of the waist and the other leg only acts as

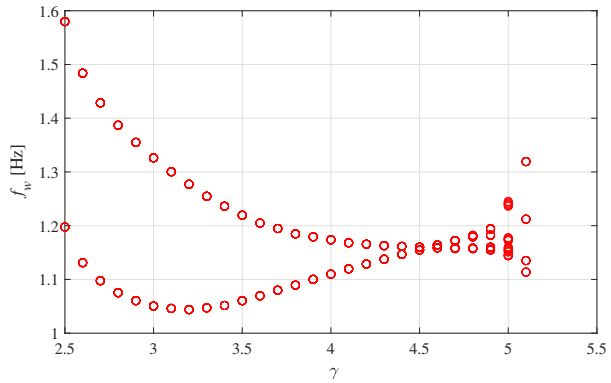

(a) Searched biped walking frequency

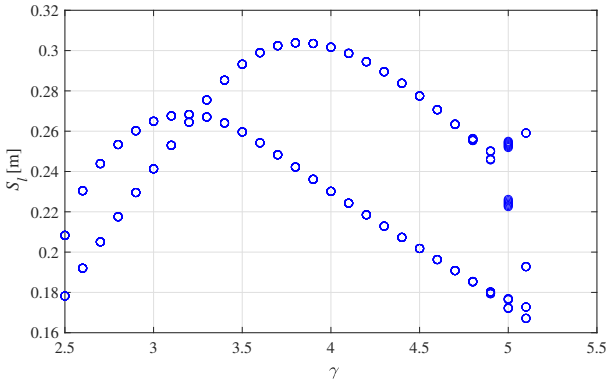

(b) Searched biped walking distance

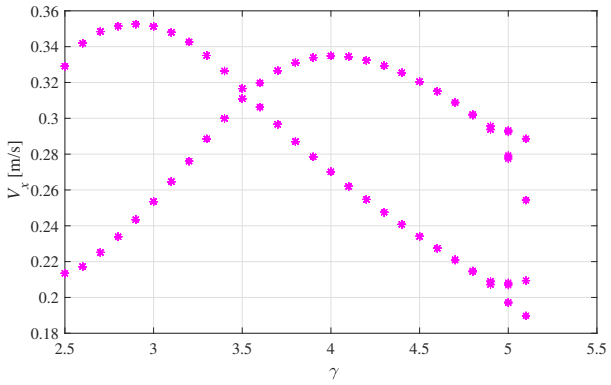

(c) Searched biped walking speed

Fig. 9. Relationships of walkable T_{set} [s]

a pendulum, under the given initial conditions, the range of the first few steps is very large, then the region is gradually stable, the angle of walking is stable in a very small state, and The stride of the legs are vary in length.

Fig. 8 shows the stick diagram of the stance leg and swing leg where $T^{\mathrm{a}}_{\mathrm{set1}}$=0.3 [s], $T^{\mathrm{s}}_{\mathrm{set1}}$=0.35 [s], $T^{\mathrm{a}}_{\mathrm{set2}}$=0.3 [s] and $T^{\mathrm{s}}_{\mathrm{set2}}$=0.35 [s] about Fig. 2, Since one more reaction wheel is added to the damaged leg, the two inputs cooperate at the same time, the stride length can be controlled, also the walking speed can be controlled. When the $T^{\mathrm{a}}_{\mathrm{set}}$=$T^{\mathrm{a}}_{\mathrm{set1}}$=0.3 [s], at the same time and under the same initial conditions, the model in Fig. 1 is still more than twice slower than that in Fig. 2.

To explore the range of target time within which robot in Fig. 1 can walk with a single input, we searched the T_{set}. Fig. 9 shows the relationships of walkable $T^{\mathrm{s}}_{\mathrm{set}}$ when the $T^{\mathrm{s}}_{\mathrm{set}} = \gamma T^{\mathrm{a}}_{\mathrm{set}}$, here the $T^{\mathrm{a}}_{\mathrm{set}}$=0.3 [s]. The multiple γ increases by 0.1 every time. It's stable to walk from about 2.5 to 5.1 times. As seen from f_w [Hz] in the Fig. 9 (a), the vertical axis represents the frequency f_w [Hz] of both legs. The walkable $T^{\mathrm{s}}_{\mathrm{set}}$ is the shortest(0.75 [s]), the frequency is the highest. Then the Fig. 9 (b) shows the walking distance S_l [m] of both legs, the longest stride is about 3.7 times. Finally, Fig. 9 (c) shows the walking speed V_x [m/s], the fastest walking speed is $T^{\mathrm{s}}_{\mathrm{set}}$=1.2 [s].

V. Conclusion and Future Work

In this paper, a biped robot with one-side passive/broken leg is stabilized using reaction wheel with appropriate actuation timing set. Through numerical simulations, we show that the influence of different target time T_{set} on the gait. We searched the range of the $T^{\mathrm{s}}_{\mathrm{set}}$ when robot has only single input. Eventually, we can control the angle of the both leg by the double reaction wheels. Therefore we can control the distance of the walking speed.

In the future work, we will verify this control technique by experimental study with a real machine. Extending the locomotion on rough terrain is also of interest.

References

[1] F. Asano, "Stealth walking of 3-link planar underactuated biped," *Proc. of the IEEE/RSJ International Conference on Intelligent Robots and Systems*, pp. 4118–4124, 2017.

[2] F. Asano, Y. Zheng, Y. Kikuchi and X. Xiao, "Generation of collisionless walking gait for non-straight-legged biped," *Proc. of the SICE Annual conference*, pp. 817–820, 2017.

[3] Y. Sakagami, R. Watanabe, C. Aoyama, S. Matsunaga, N. Higaki and K. Fujimura, "The intelligent ASIMO: system overview and integration," *Proc. of the IEEE/RSJ International Conference on Intelligent Robots and Systems*, vol. 3, pp. 2478–2483, 2002.

[4] S. Kuindersma, R. Deits, M. Fallon, A. Valenzuela, H. Dai, F. Permenter, T. Koolen, P. Marion and R. Tedrake, "Optimization-based locomotion planning, estimation, and control design for the atlas humanoid robot," *Autonomous Robots*, vol. 40, pp. 429–455, 2016.

[5] T. Brown and J. Schmiedeler, "Gait transitions and disturbance response for planar bipeds with reaction wheel actuation," *Proc. of the IEEE/RSJ International Conference on Intelligent Robots and Systems*, pp. 3393–3398, 2016.

[6] T. Brown and J. Schmiedeler, "Reaction wheel actuation for improving planar biped walking efficiency," *IEEE Transactions on Robotics*, vol.32, no. 5, pp. 1290–1297, 2016.

[7] T. Brown and J. Schmiedeler, "Energetic effects of reaction wheel actuation on underactuated biped robot walking," *Proc. of the IEEE/RSJ International Conference on Robotics and Automation*, pp. 2576–2581, 2014.

[8] T. McGeer, "Passive dynamic walking," *International Journal of Robotics Research*, vol. 9, no. 2, pp. 62–82, 1990.

[9] T. McGeer, "Passive walking with knees," *Proc. of the IEEE Conference on Robotics and Automation*, vol. 2, pp. 1640–1645, 1990.